Soft Matter

Dynamic Article Links

Cite this: *Soft Matter*, 2011, **7**, 3286

www.rsc.org/softmatter

COMMUNICATION

Effect of the volume fraction of solids on the concentration polarization around spheroidal hematite particles

Raúl A. Rica,* María L. Jiménez and Ángel V. Delgado

Received 29th January 2011, Accepted 25th February 2011
DOI: 10.1039/c1sm05153a

We present the first experimental results on the effect of the particles content (up to $\phi = 20\%$ volume fraction of solids) in the low frequency dielectric dispersion (LFDD) of suspensions of hematite (α-Fe_2O_3) prolate spheroidal colloids. Two α-relaxations, each one associated to a characteristic dimension of the particles, are clearly observed, but they present different dependencies with volume fraction. Accounting for particle–particle interactions, in terms of models for spheres, allows a comprehensive interpretation of the mechanisms involved, suggesting the presence of a nematic phase in our suspensions.

Electrokinetics of dilute suspensions is a well established field that has been widely investigated both theoretically and experimentally in multiple conditions. However, when the solids concentration is high enough for particle–particle interactions to be significant, the electrokinetic behaviour starts to be uncharted. This is partly due to the theoretical ravel that their inclusion involves, and partly due to the limited experimental approachability. In this context, recent theoretical advances[1,2] and experimental results[3,4] are clear examples of the success of cell models in the description of spherical and oblate particle systems. The electrokinetic characterization of such highly concentrated suspensions can be carried out using either electroacoustic or dielectric techniques. In both cases, alternating fields are applied because the frequency dependence of the measured quantity is also very informative. The former technique allows the evaluation of the frequency-dependent electrophoretic mobility (the so-called dynamic mobility). In dielectric experiments, the frequency (ν) dispersion of the electric permittivity of the suspensions is the phenomenon of interest, as long as the frequency sweep includes the regions where relaxations in the double layer polarization can occur. We have recently proposed a semianalytical approximation for the dynamic mobility and electric permittivity spectra of prolate particles, and the model was applied to experimental results obtained on relatively polydisperse goethite suspensions.[5,6] In this contribution, our purpose is to describe novel experimental results on the low frequency dielectric dispersion (LFDD) of even higher concentrations (up to 20% v/v) of prolate, monodisperse hematite particles (α-Fe_2O_3).

Department of Applied Physics, School of Sciences, University of Granada, 18071 Granada, Spain. E-mail: rul@ugr.es; Tel: +34-958243209

In the LFDD electrokinetic technique, the real and imaginary components of the relative permittivity of the disperse system $\varepsilon^*(\nu) = \varepsilon'(\nu) - i\varepsilon''(\nu)$ are obtained from data on the AC conductivity of the systems. As is well known for the case of spheres,[7] the main feature of the dielectric spectrum of colloidal suspensions is a strong decrease in $\varepsilon'(\nu)$ and a subsequent maximum in $\varepsilon''(\nu)$ when the frequency is increased above a critical value ν_α, associated to the disappearance of the concentration polarization of the double layer. This is the accumulation of neutral electrolyte on one pole of the particle in the field direction, and depletion on the other. The characteristic distance for the formation of such clouds is of the order of the particle dimensions, meaning that for frequencies above $\nu_\alpha \sim D/a^2$, where D is the average diffusion coefficient of ions in solution and a is the particle radius, polarization cannot occur. This is the phenomenon of α-dispersion, and it is responsible for the shift of high to low permittivities shown by disperse systems at low frequencies.

The hematite particles were synthesized through hydrolysis of iron(III) chloride solutions at 100 °C.[8] Their size and shape were characterized by dynamic light scattering (hydrodynamic radius $R_H = 130 \pm 30$ nm) and SEM pictures (semiaxes $a = 276 \pm 18$ nm, $b = 45 \pm 6$ nm, see Fig. 1). Prior to any analysis, the synthesized particles were cleaned by successive cycles of centrifugation and redispersion in deionized and filtered water (Milli-Q Academic, Millipore, France) until the conductivity of the supernatant was below 1 μS cm^{-1}. In order to avoid the *suspension effect* of the particles when measuring the pH in suspensions containing large concentrations of solids,[9] the preparation of the samples was as follows: once the suspension was clean, the centrifugation–redispersion procedure was repeated with a 0.5 mM KNO_3 solution at a given pH until the pH of the supernatant reached a constant value. The volume of the final suspension was controlled to reach the highest concentration of solids ($\phi = 20\%$). Suspensions with lower

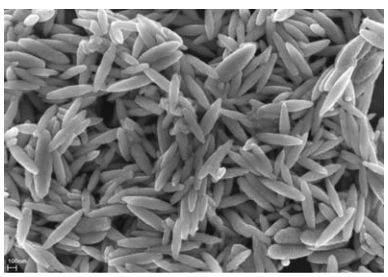

Fig. 1 The SEM picture of the hematite particles.

volume fractions were prepared by dilution from this one with the same solution, while the pH of the supernatant was tested every two dilution steps. Two values of the pH of the ionic solution were used, namely 3.5 and 3.7, and the obtained suspensions always had pH values 3.7 ± 0.1 and 4.0 ± 0.1, respectively.

The permittivity spectra of the suspensions were obtained by measuring the frequency dependence (in the 1 kHz–1 MHz range) of the impedance of a conductivity cell with parallel, platinised-platinum electrodes at 25 ± 0.5 °C, with the measured suspension between them, using an HP 4284A (USA) impedance meter.[10] Typically, the applied electric field strength was 50 mV cm^{-1}. The main limitation when performing low-frequency impedance spectroscopy in aqueous media is the phenomenon of electrode polarization (EP), which may add a contribution to the measured impedance in the kHz frequency range, partially masking the signal coming from the particle-solution interface. Among other existing methods,[10,11] the *logarithmic derivative* technique has been shown to be able to properly eliminating, to a large extent, the perturbing contribution of electrode polarization.[12,13] The logarithmic derivative of the real part of the relative permittivity $\varepsilon'(\nu)$ is $\varepsilon_D'' = -\pi/2(\partial\varepsilon'/\partial\ln\nu)$. This quantity displays a frequency dependence similar to that of the imaginary part of the electric permittivity ($\varepsilon_D''(\nu) \simeq \varepsilon''(\nu)$), but, interestingly, the electrode contribution ε_D'' falls with frequency more rapidly than its contribution to ε'', and this makes it easier to eliminate or minimise the electrode polarization contribution. Furthermore, the real component of the permittivity can be obtained by numerical integration. As an example, the symbols in Fig. 2 (a) show the uncorrected logarithmic derivative spectra for the indicated values of the volume fraction of solids of the suspensions at pH 4. The linear decay at low frequency is the EP contribution. In this plot, the lines are fitted to the low-frequency ($\nu < 1$ kHz) part of these spectra, properly catching the contribution of EP. By subtracting these lines from the full spectra, we obtain the data shown in Fig. 2b.

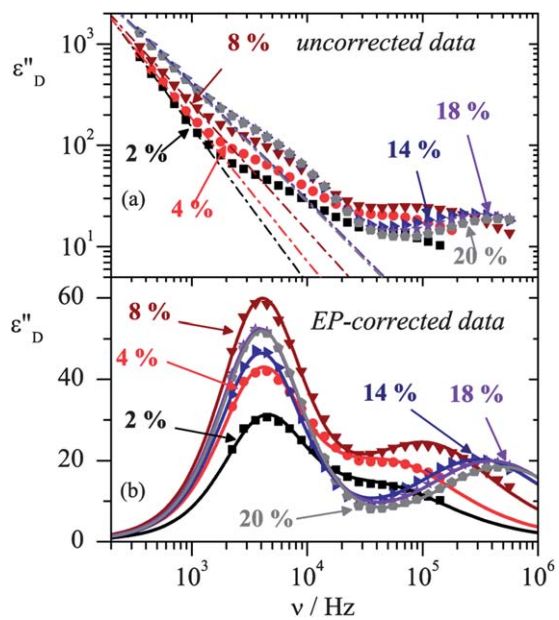

Fig. 2 (a) Symbols: spectra of the logarithmic derivative of the relative permittivity of suspensions of hematite particles in 0.5 mM, pH 4.0 ± 0.1 solutions, for the indicated values of the volume fraction of the solids (ϕ). Lines: fits of the low-frequency ($\nu < 1$ kHz) portions of the spectra. (b) Symbols: the same as (a), but for the EP-corrected data. Lines: best fits to the logarithmic derivative of a combination of two Cole-Cole relaxation functions, eqn (2).

After the data have been corrected from the EP contribution, we observe two relaxation peaks instead of the single one encountered for spherical particles.[6] These peaks are fitted with the logarithmic derivative of a frequency dispersion function consisting of two Cole-Cole relaxations,[14] using a non-linear fit procedure. To that aim, a complex dielectric increment, $\Delta\varepsilon^*(\nu)$, accounting for the role of dispersed particles on the overall relative permittivity, is first defined as follows:

$$\varepsilon^*(\nu) = \varepsilon_m + \Delta\varepsilon^*(\nu) \quad (1)$$

where ε_m is the relative permittivity of the dispersion medium. Since ε_m is constant for the investigated frequency range, $\varepsilon_D'' = \Delta\varepsilon_D'' = -\pi/2(\partial\Delta\varepsilon'/\partial\ln\nu)$. The dielectric increment is then described in terms of a double Cole-Cole function:

$$\Delta\varepsilon^*(\nu) = \frac{\Delta\varepsilon_{LF}}{1 + (j\nu/\nu_{LF})^{1-\gamma_{LF}}} + \frac{\Delta\varepsilon_{HF}}{1 + (j\nu/\nu_{HF})^{1-\gamma_{HF}}} \quad (2)$$

Here, ν_{LF} and ν_{HF} are the characteristic frequencies of the low- and high-frequency relaxations, respectively, whose amplitude is expressed by the dielectric increments $\Delta\varepsilon_{LF}$ and $\Delta\varepsilon_{HF}$. $\gamma_{LF,HF}$ are parameters of the respective Cole-Cole functions, indicating their width. Note that, in the fitting procedure, it is not possible to discriminate between the two peaks for the lowest values of ϕ, as they are very close to each other. However, we found that those curves where the two relaxations are well separated, can be fitted with the values $\gamma_{LF} = 0.05$ and $\gamma_{HF} = 0.28$. We selected these two γ values for the whole data set and did not vary them. In the case of pH 3.7, the values are slightly different: $\gamma_{LF} = 0.1$ and $\gamma_{HF} = 0.19$.

Let us qualitatively analyse the behaviours observed in Fig. 2b. The derivative spectra show clearly two maxima that are better resolved the larger the particle concentration, due to their different tendencies. Regarding the low-frequency (LF) relaxation process, the amplitude of the dielectric increment goes through a maximum and reaches a plateau when the volume fraction of solids is increased. The high-frequency (HF) relaxation also describes a maximum in the amplitude, but beyond it the amplitude of the relaxation decreases. Moreover, a concomitant increase of the characteristic frequency (ν_{HF}) with volume fraction is observed.

A quantitative description of the main features of the dielectric relaxation of spheroids, just described, can be made possible by fitting the data to the logarithmic derivative of eqn (2). From the fits, the data in Fig. 3 were obtained. Fig. 3a and Fig. 3b show the dielectric increments $\Delta\varepsilon_{LF,HF}$ at pH values 3.7 and 4, respectively, and Fig. 3c includes the characteristic frequencies of the Cole-Cole distributions. From the first two plots, we note that already at $\phi \simeq 0.02$ the dielectric increment departs from a linear dependence with ϕ. After this linear region, a local maximum is seen in the values of both the LF and HF dielectric increments, but the LF tends to a plateau as ϕ is increased while the HF one continues with a decreasing trend in the measured range. On the other hand, the behaviours of the characteristic frequencies in the LF and HF cases are very different: while the former has an almost constant value $\nu_{LF} \simeq 4$ kHz (value obtained by fitting the data to an horizontal line), the HF one experiences an increase from $\nu_{HF} \simeq 40$ kHz to $\nu_{HF} \simeq 600$ kHz, that is, a shift of more than one order of magnitude.

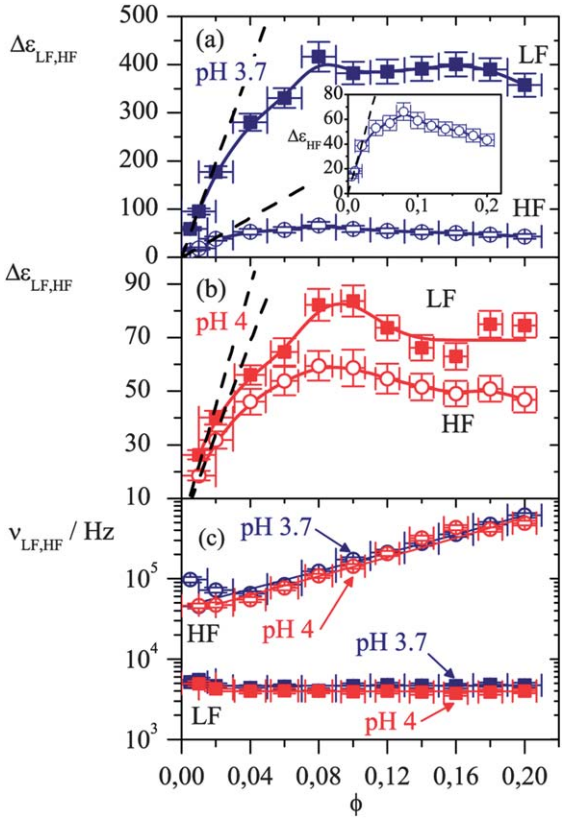

Fig. 3 Full squares: LF data. Open circles: HF data. (a) Value of the dielectric increment obtained from the fits of data in Fig. 2b (pH 3.7) to eqn (2) with $\gamma_{LF} = 0.1$ and $\gamma_{HF} = 0.19$. Dashed lines: fits to a linear model of the data with $\phi < 0.02$. Full lines are a guide to the eye. The inset is a zoom of the HF curve. (b) Value of the dielectric increment obtained from fitting the data at pH 4 to eqn (2) with $\gamma_{LF} = 0.05$ and $\gamma_{HF} = 0.28$. Dashed lines: fits to a linear model of the data with $\phi < 0.02$. Full lines are a guide to the eye. (c) The same as (a), but for the values of the characteristic frequency and both values of pH. The lines here are the best fits to eqn (6).

No theoretical models are available for the description of the dielectric spectroscopy of concentrated suspensions of spheroids. First of all, even in the case of dilute systems, orientation effects must be taken into account, considering that, the polarization of the EDL of spheroids will be different for parallel and perpendicular orientations. The problem was solved by Grosse *et al.*[15] for dilute suspensions, who assumed Debye-like relaxations of the permittivity for each particle orientation:

$$\varepsilon_d^{*,i}(\nu) = \varepsilon_m + \phi\delta\varepsilon_d^{*,i}(\nu) = \varepsilon_m + \phi\frac{\delta\varepsilon_d^i(0)}{1 + j\nu/\nu_{\alpha,d}^i} \quad (3)$$

where $\delta\varepsilon_d^i(0)$ is the dielectric increment per unit volume fraction, and a linear dependence on the particle concentration ϕ is assumed, as expected for the dilute case. The superscript $i = \|, \perp$ corresponds, respectively, to the parallel and perpendicular orientations of the symmetry axis of the spheroid with respect to the field. Keeping in mind that measurements are typically carried out for randomly oriented spheroids in suspension, the dielectric increments for both orientations must be combined for the random distribution as follows:

$$\delta\varepsilon_d^*(\nu) = \frac{\delta\varepsilon_d^{*,\|}(\nu) + 2\delta\varepsilon_d^{*,\perp}(\nu)}{3} \quad (4)$$

This expression allows us to assign the two relaxations observed in Fig. 2b to the separate contributions of the EDL relaxations for parallel and perpendicular orientations, that is, the α-dispersions associated to each semi-axis of the spheroids.

The effect of particle volume fraction will be considered following a mixed treatment[6] in which the Grosse *et al.* model just described for diluted suspensions was complemented with a semi-quantitative correction for the effect of a finite volume fraction in the case of spheres.[16] In spite of its limitations, these results demonstrated that the method catches most of the features of the permittivity of spheroidal particle suspensions. In addition, full numerical solution of the problem in the case of spheres[2] showed very good agreement with the predictions of the specific dielectric increment ($\delta\varepsilon$) and α-relaxation frequencies, as expressed by the following equations:

$$\delta\varepsilon^i(\phi) = \delta\varepsilon_d^i\left(1 + \frac{1}{\left(\phi^{-1/3} - 1\right)^2}\right)^{-3/2} \quad (5)$$

$$\nu_\alpha^i(\phi) = \nu_{\alpha,d}^i\left(1 + \frac{1}{\left(\phi^{-1/3} - 1\right)^2}\right) \quad (6)$$

These equations predict a local maximum in the $\Delta\varepsilon - \phi$ relationship, followed by a monotonous decrease, while ν_α shows a monotonous increase. The physical origin of these trends lies on the overlapping of the concentration polarization ionic clouds of the different particles. On the one hand, when two particles are close enough, the ion-enriched region of one particle will balance the ion-depleted region of its neighbour, partially cancelling the perturbations on the local concentration and diminishing the fluxes that lead to the large LF values of the electric permittivity. On the other hand, the ionic diffusion lengths are shortened when particles approach each other, thus decreasing the characteristic time of the process.

According to data in Fig. 3, only the high frequency behaviour qualitatively agrees with the predictions of eqn (5) and (6), but quantitative agreement is unreachable in both cases. In fact, fitting our data to these equations leads to statistically non significant parameters. However, if ϕ is substituted by an "effective volume fraction" $\phi_{eff} = f \times \phi$ in eqn (5) and (6), the data can be fitted

Table 1 Best-fit parameters of the data in Fig. 3 to eqn (5) and (6) ("Sphere model"), and to the equation $\Delta\varepsilon(\phi) = \delta\varepsilon_d \times \phi$ ("Linear model"). $f_{\delta\varepsilon}$ and f_ν are the values of f obtained by fitting the data of $\delta\varepsilon$ and $\nu_\alpha$to eqn (5) and (6).

	pH 3.7		pH 4	
Sphere model				
	$\delta\varepsilon_d$	$f_{\delta\varepsilon}$	$\delta\varepsilon_d$	$f_{\delta\varepsilon}$
LF	9900 ± 400	1.06 ± 0.04	2350 ± 210	1.30 ± 0.10
HF	2130 ± 120	1.47 ± 0.06	1900 ± 100	1.37 ± 0.06
	$\nu_{\alpha,d}$/kHz	f_ν	$\nu_{\alpha,d}$/kHz	f_ν
LF	4.66 ± 0.23	0 ± 5 × 10^{-6}	3.96 ± 0.12	0 ± 5 × 10^{-6}
HF	43 ± 4	2.42 ± 0.15	36 ± 3	2.52 ± 0.12
Linear model				
	$\delta\varepsilon_d$		$\delta\varepsilon_d$	
LF	9900 ± 400		2200 ± 300	
HF	2040 ± 140		1710 ± 130	

satisfactorily, leading to the parameters in Table 1 ("Sphere model"). Here, f is a factor including information about the geometry of the particles (note that the considered model was developed for spheres), and which can be in principle different for different orientations.

We can also consider the linear range of $\Delta\varepsilon - \phi$ plots in Fig. 3a, where the particles are far enough from each other as to make their interactions negligible. These linear ranges were fitted to an equation of the type $\Delta\varepsilon = \delta\varepsilon_d \times \phi$, and therefore the value of "$\delta\varepsilon_d$" can be extracted, as indicated in Table 1 ("Linear model").

Note that the particles are less charged at pH 4 than 3.7,[8,17] and this explains the larger $\delta\varepsilon$ in the later case. In addition, the effect of pH variations on the characteristic frequency of the relaxation is negligible, as this is controlled by D and the size. Because of the above mentioned relationship between the characteristic α-relaxation frequency and the particle dimension in the case of spheres, we ascribe the LF (HF) parameters to the long (short) semi-axis of the spheroids. In other words, $\Delta\varepsilon_{LF}$ would be the dielectric amplitude for the parallel orientation, that is, the particles oriented with their long semi-axis in the direction of the field. Similarly, HF would correspond to the perpendicular orientation.

Perhaps the most unexpected finding presented is how the content of solids affects the characteristic frequency of the LF α-relaxation. The proved (both theoretically and experimentally) increase in α-frequency with ϕ in the case of spheres (and in the perpendicular orientation of our particles) is completely absent in the LF relaxation peak, in turn giving a zero value for the parameter f. Note that this cannot be explained by assuming that the volume fraction is low so that the particles are far from each other on average, as we do observe an effect on the dielectric increment (*i.e.*, the plateau its value achieves). We attribute this finding to the possible presence of a nematic phase in our suspensions (perhaps, field induced, like in recent experiments with fd-viruses,[11] that are similar in size and shape to our particles), although an experimental confirmation with a different technique is necessary. If a nematic phase were present, where the spheroids are locally aligned (but the overall orientation is random), lateral interactions would be more likely to occur amongst the particles, thus the effects of ϕ on the HF relaxation process would be more apparent, as was observed. In fact, the relative contribution to the total polarization of each LF and HF dielectric increment is not constant, but the weight of the former increases with ϕ in almost the whole range of volume fractions studied (in particular, the ratio $\Delta\varepsilon_{LF}/\Delta\varepsilon_{HF}$), suggesting that lateral concentration polarization (manifested in HF) is more strongly cancelled by interactions between particles. Regarding the value of $\nu_{\alpha,LF}$, it is not manifestly affected by ϕ for the same reason, as the concentration polarization clouds occupy mainly the regions of solution in the direction of the symmetry axis.

Summarizing, we have presented a set of experimental data regarding the effect of solid contents on the LFDD of suspensions of prolate monodisperse colloidal hematite. The very rich physical phenomenology observed, showing features absent in suspensions of spheres, offers unique possibilities to study and characterize concentrated suspensions of non-spherical colloids. In particular, the presence of two separate α-processes has been confirmed, each one associated to a characteristic dimension of the particles, and the effects of inter-particle interactions on their behaviour have been illustrated. Qualitative agreement of this behaviour with models for spheres was found, but some features require theoretical developments, specific for the interactions of spheroidal particles. Finally, the demeanour of the LF relaxation process with ϕ suggests the presence of a nematic phase in our suspensions, but experimental confirmation with a different technique is desirable.

Acknowledgements

Financial support from the Spanish Ministry of Education (for a FPU grant to RAR) and Junta de Andalucía (Spain) project PE-2008-FQM3993 is gratefully acknowledged.

References

1 S. Ahualli, A. Delgado, S. J. Miklavcic and L. R. White, *Langmuir*, 2006, **22**, 7041–7051.
2 F. Carrique, F. J. Arroyo, M. L. Jimenez and A. V. Delgado, *J. Chem. Phys.*, 2003, **118**, 1945–1956.
3 M. Guerin and J. C. Seaman, *Clays Clay Miner.*, 2004, **52**, 145–157.
4 S. Ahualli, M. Jimenez, A. Delgado, F. Arroyo and F. Carrique, *IEEE Trans. Dielectr. Electr. Insul.*, 2006, **13**, 657–663.
5 R. A. Rica, M. L. Jimenez and A. V. Delgado, *Langmuir*, 2009, **25**, 10587–10594.
6 R. A. Rica, M. L. Jimenez and A. V. Delgado, *J. Colloid Interface Sci.*, 2010, **343**, 564–573.
7 C. Grosse and A. V. Delgado, *Curr. Opin. Colloid Interface Sci.*, 2010, **15**, 145–159.
8 M. P. Morales, T. Gonzalez-Carreño and C. J. Serna, *J. Mater. Res.*, 1992, **7**, 2538–2545.
9 S. F. Oman, M. F. Camoes, K. J. Powell, R. Rajagopalan and P. Spitzer, *Pure Appl. Chem.*, 2007, **79**, 67–79.
10 M. C. Tirado, F. J. Arroyo, A. V. Delgado and C. Grosse, *J. Colloid Interface Sci.*, 2000, **227**, 141–146.
11 K. Kang and J. K. G. Dhont, *Soft Matter*, 2010, **6**, 273–286.
12 M. L. Jimenez, F. J. Arroyo, J. van Turnhout and A. V. Delgado, *J. Colloid Interface Sci.*, 2002, **249**, 327–335.
13 P. A. Cirkel, J. P. M. van der Ploeg and G. J. M. Koper, *Phys. A*, 1997, **235**, 269–278.
14 K. S. Cole and R. H. Cole, *J. Chem. Phys.*, 1941, **9**, 341–351.
15 C. Grosse, S. Pedrosa and V. N. Shilov, *J. Colloid Interface Sci.*, 1999, **220**, 31–41.
16 A. V. Delgado, F. J. Arroyo, F. Gonzalez-Caballero, V. N. Shilov and Y. B. Borkovskaya, *Colloids Surf., A*, 1998, **140**, 139–149.
17 M. L. Jimenez, F. J. Arroyo, F. Carrique and U. Kaatze, *J. Phys. Chem. B*, 2003, **107**, 12192–12200.